# *Supporting Information*

## Mixed salts $NH_4Cl$-NaCl assisted pyrolysis route for preparation of high performance Fe/N/C oxygen reduction reaction catalyst

*Kun Hou[a], Zhen Sun[a], Lunhui Guan*[a]*

a. CAS Key Laboratory of Design and Assembly of Functional Nanostructures, and Fujian Key Laboratory of Nanomaterials, Fujian Institute of Research on the Structure of Matter, Chinese Academy of Sciences, Fuzhou, Fujian 350002, China.

† Corresponding author: guanlh@fjirsm.ac.cn (L.H. Guan)

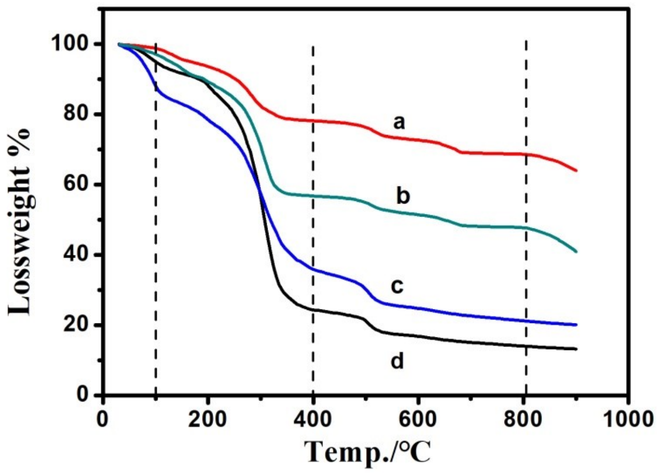


**Figure S1** The thermogravimetric analysis curves of the Fe/N/C catalysts: a) Fe/N/C-NaCl; b) Fe/N/C-$NH_4Cl$/NaCl; c) Fe/N/C-PmPDA; d) Fe/N/C-$NH_4Cl$. The weight loss below 100 $^{o}$C can be attributed to the physically absorbed water. The samples with $NH_4Cl$ added experience a more drastic weight loss between 100 $^{o}$C and 400 $^{o}$C due to the decompositon of $NH_4Cl$ in this temperature domain. All the measurments were carried out under nitrogen and the ramping rate was 10 $^{o}$C/min

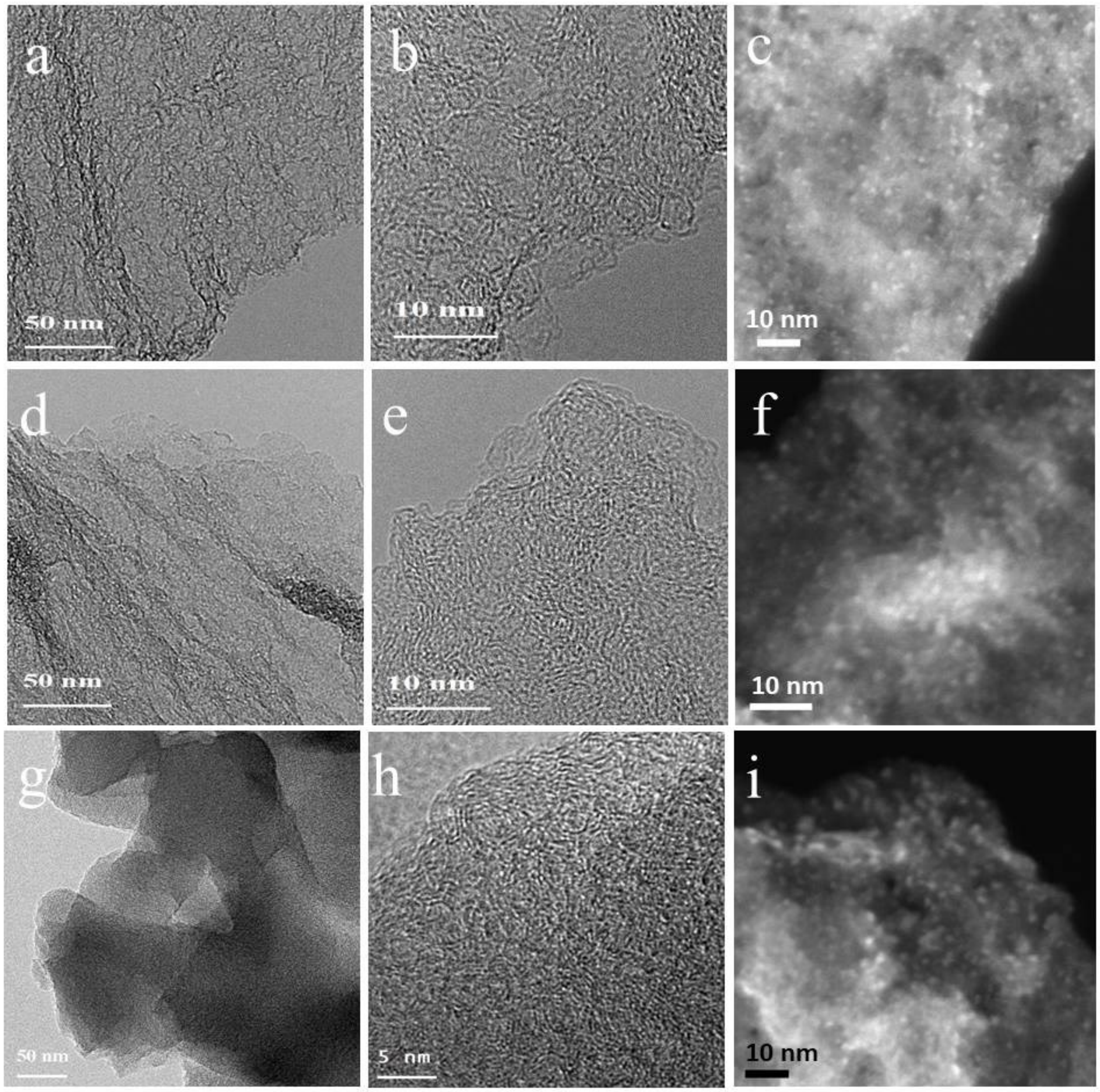


**Figure S2** The TEM and HAADF-STEM images of samples Fe/N/C-NaCl, a-c; Fe/N/C-$NH_4Cl$, d-f; and Fe/N/C-PmPDA, g-i.

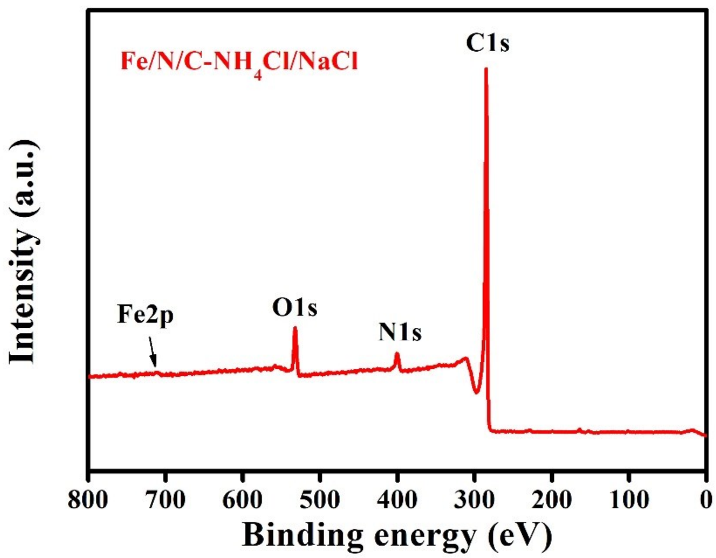


**Figure S3** The XPS survey spectrum of Fe/N/C-$NH_4Cl$/NaCl catalyst

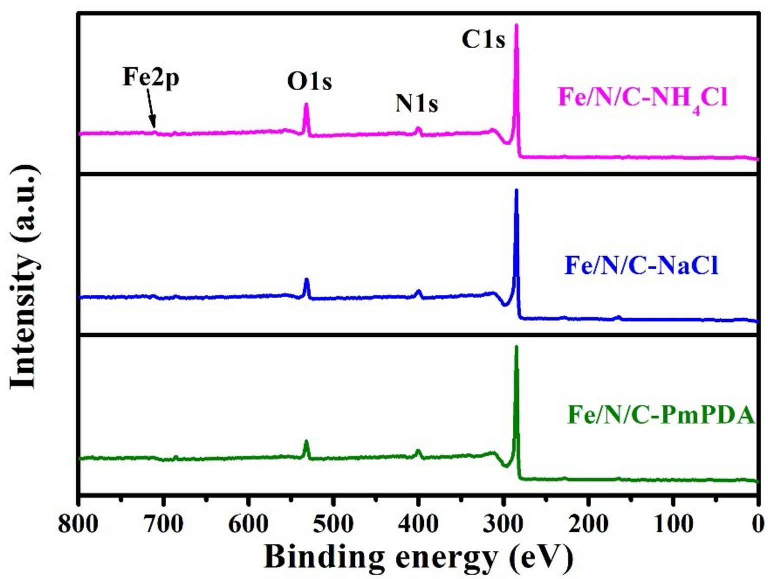


**Figure S4** XPS survey spectra of Fe/N/C-PmPDA, Fe/N/C-$NH_4Cl$ and Fe/N/C-NaCl catalysts.

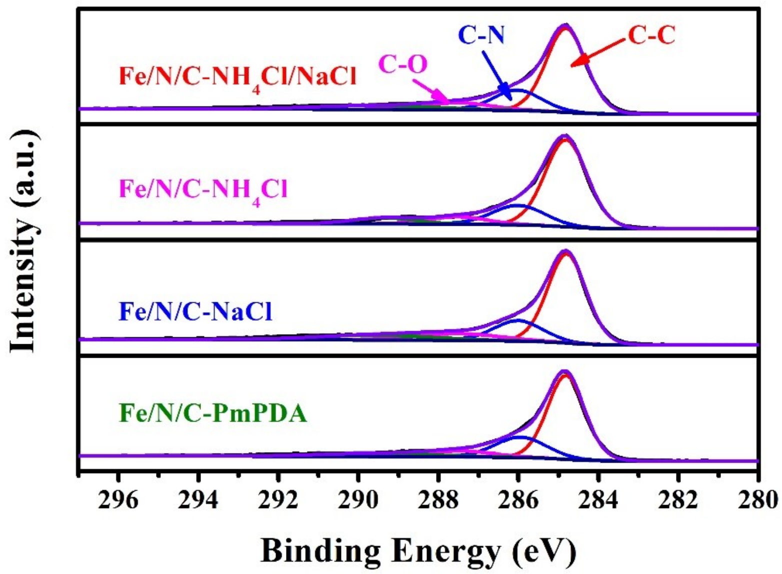


**Figure S5** C1s XPS spectra of Fe/N/C-PmPDA, Fe/N/C-$NH_4Cl$, Fe/N/C-NaCl and Fe/N/C-$NH_4Cl$/NaCl.

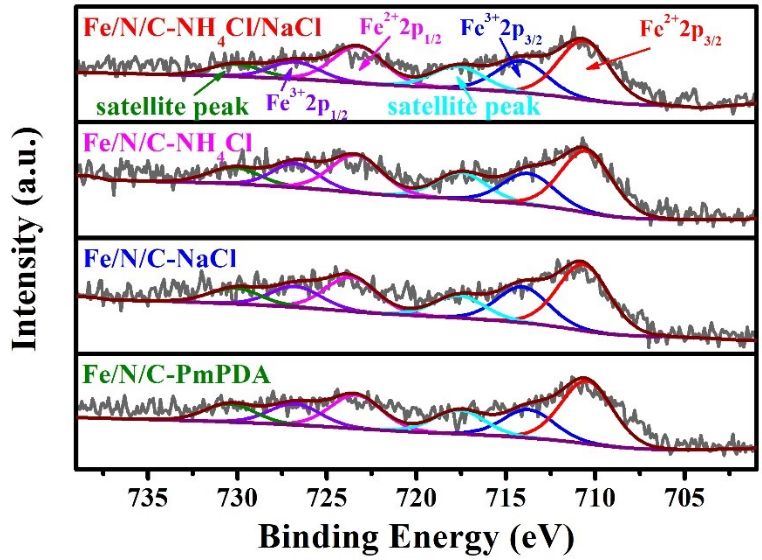


**Figure S6** Fe 2p XPS spectra of Fe/N/C-PmPDA, Fe/N/C-$NH_4Cl$, Fe/N/C-NaCl and Fe/N/C-$NH_4Cl$/NaCl.

**Table S1.** The elemental quantification analysis of the C, O, Fe, N atomic ratios in different Fe/N/C samples

| Samples | C (at%) | O (at%) | Fe ( at%) | N (at%) | Fe-Nx (at%) |
|---|---|---|---|---|---|
| **Fe/N/C-$NH_4Cl$/NaCl** | 87.48 | 6.07 | 0.65 | 5.83 | 0.56 |
| **Fe/N/C-$NH_4Cl$** | 84.94 | 9.24 | 0.55 | 5.28 | 0.35 |
| **Fe/N/C-NaCl** | 87.56 | 6.67 | 0.54 | 5.26 | 0.32 |
| **Fe/N/C-PmDA** | 88.21 | 6.60 | 0.48 | 4.72 | 0.15 |

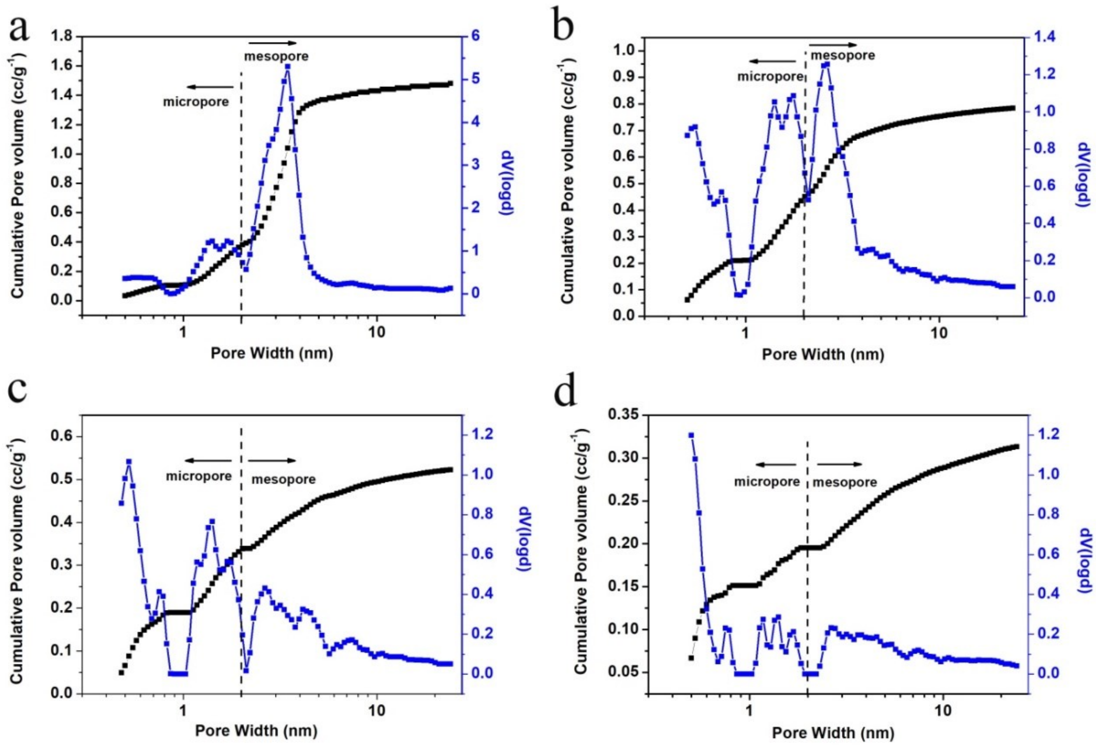


Figure S7 The pore size distribution of the Fe/N/C catalysts calculated by DFT method assuming a slit pore configuration, a) Fe/N/C-$NH_4Cl$/NaCl, b) Fe/N/C-NaCl, c) Fe/N/C-$NH_4Cl$, d) Fe/N/C-PmPDA.

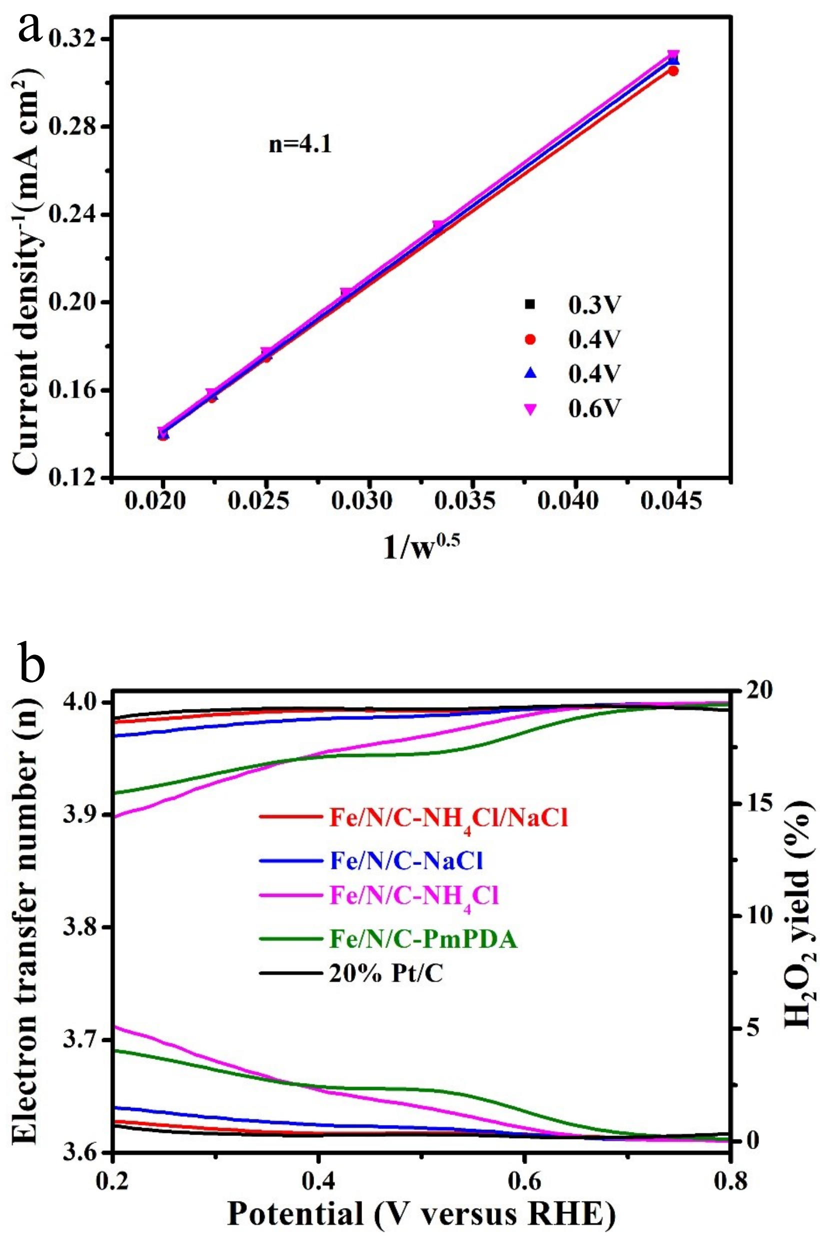


**Figure S8** a) K-L plots at different potentials, b) The electron-transfer number and $H_2O_2$ yield of different catalysts in the potential range of 0.2 to 0.8 V in 0.1 M KOH solution.

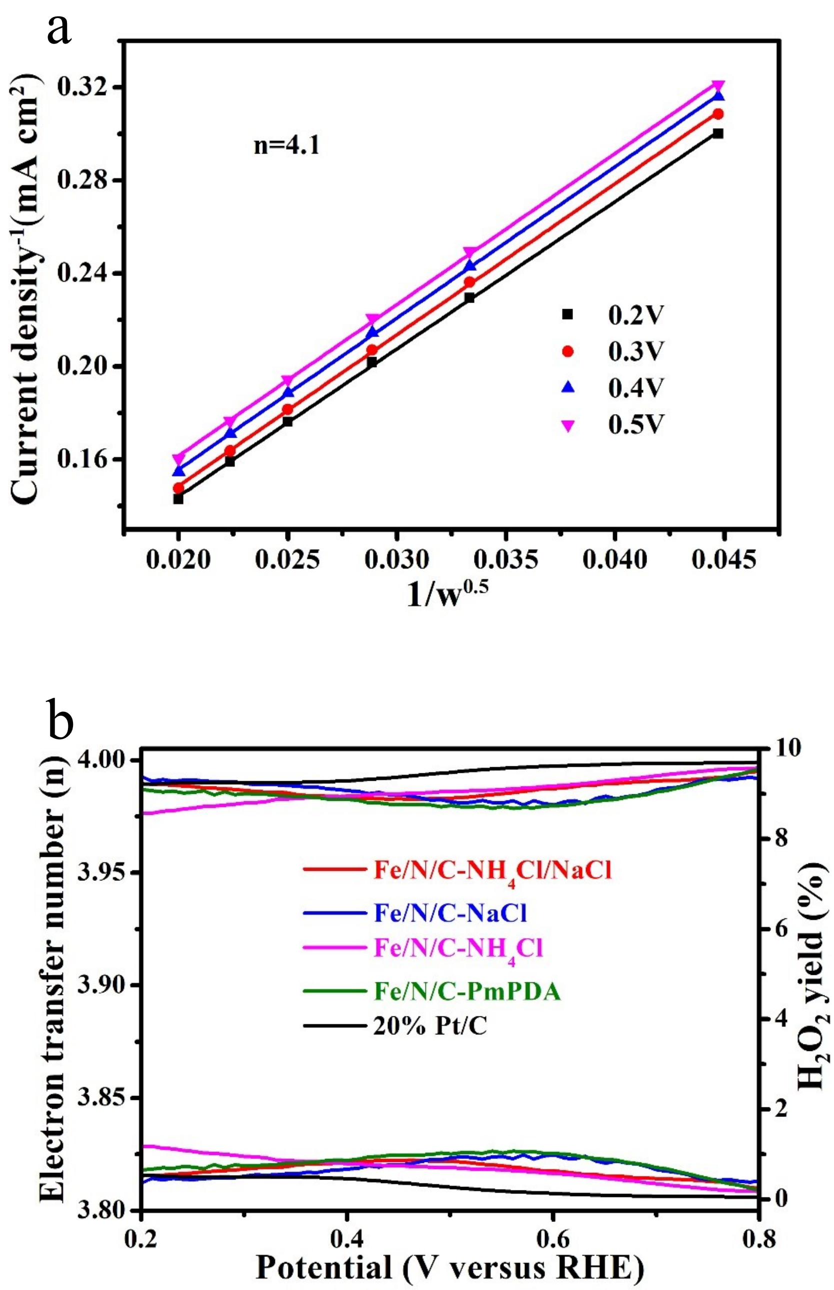


**Figure S9** a) K-L plots at different potentials, b) The electron-transfer number and $H_2O_2$ yield of different catalysts in the potential range of 0.2 to 0.8 V in 0.1 M $HClO_4$ solution.

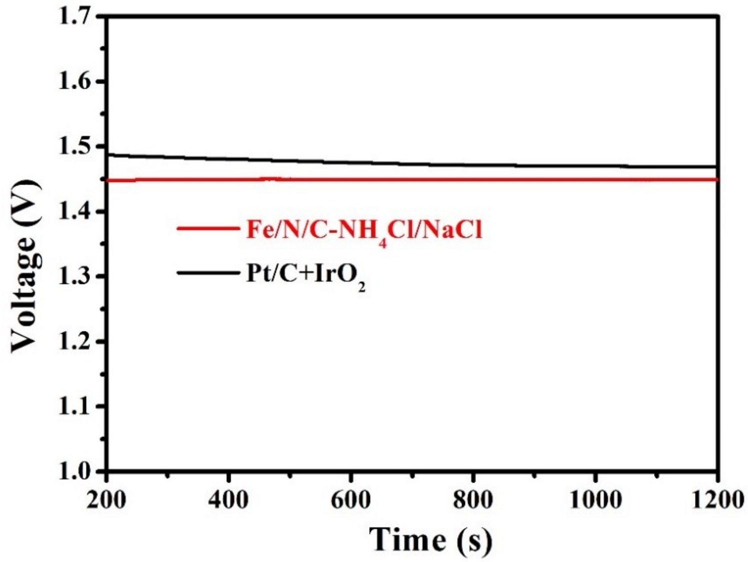


**Figure S10** Plots showing the evolution of open-circuit voltage of Zn-air batteries employing Fe/N/C-$NH_4Cl$/NaCl and Pt/C+$IrO_2$ catalysts as air cathodes.

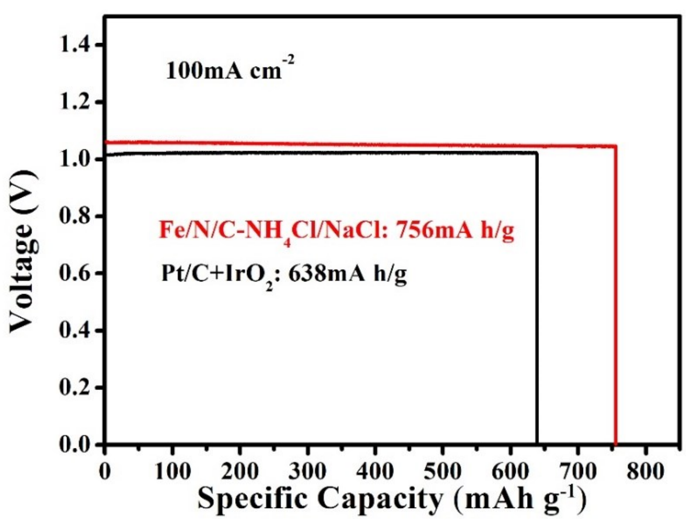


**Figure S11** Discharge curves of Zn-air batteries assembled with Fe/N/C-$NH_4Cl$/NaCl and Pt/C+$IrO_2$ catalysts as cathode at 100 mA $cm^{-2}$ discharging rate.

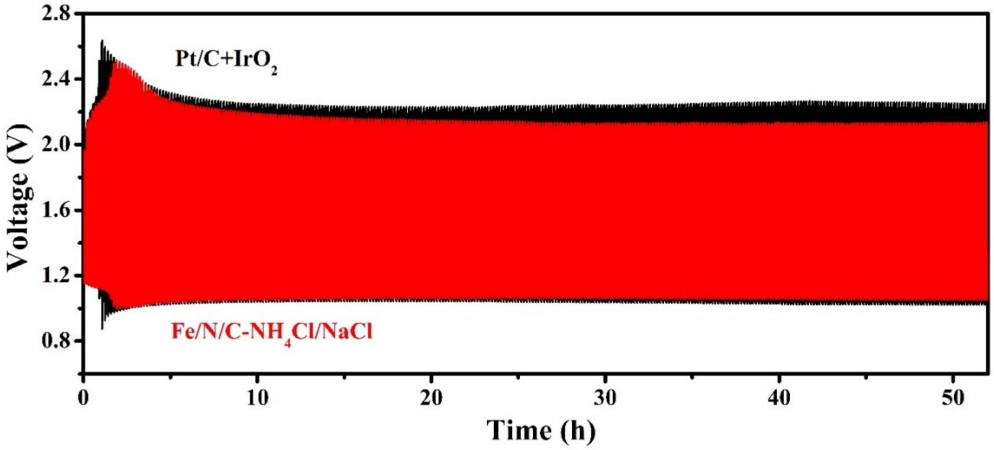


**Figure S12** Continuously charge and discharge of Zn-air batteries with different air cathodes for 52 h at 10 mA cm$^{-2}$. Both the discharge and charge intervals were set for 300 s.

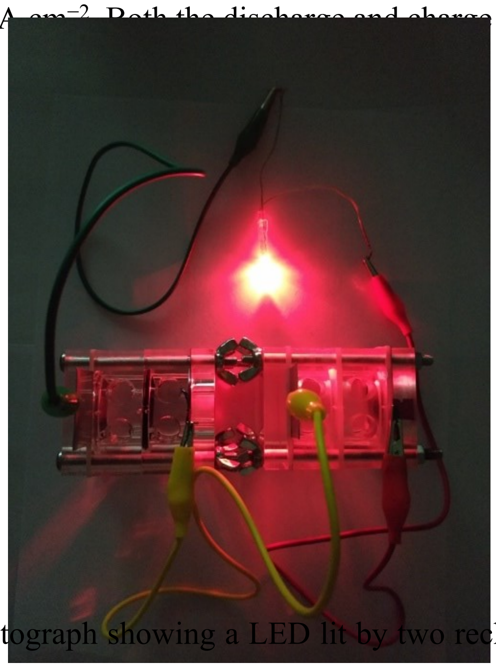

**Figure S13** This is a photograph showing a LED lit by two rechargeable Zn-air batteries connected in series.